Contribution from the Department of Chemistry,
The Ohio State University, Columbus, Ohio 43210

An Investigation of an Enzyme Model. The Influence of Solvent on the Metal-Ion-Catalyzed Decarboxylation of Oxalacetate

HSIANG-KUEN MAO and DANIEL L. LEUSSING*

Received February 26, 1981

The decarboxylation of oxalacetate (oxac) as catalyzed by Mg(II), Mn(II), and Zn(II) has been extensively studied in 1:1 (v/v) dioxane–water solvent mixtures. Briefer investigations were also made in 1:3 and 3:1 solvents. After correction for the pH effects and buffer complexation, the principal features of the reactions were found to be the same as those previously uncovered in aqueous media: decarboxylation is promoted via the formation of a 1:1 M^{II}–$oxac^{2-}$ complex while inhibition arises from the formation of mono- and dinuclear enolate complexes. The overall stability constants of the complexes show a much larger solvent effect than their decarboxylation rate constants; however, after correction for changes in the enol/keto ratios of the metal ion–oxac complexes, the true rate constants for the loss of CO_2 from the keto complexes were found to increase by about 1 order of magnitude in going from an aqueous to 50% dioxane medium. Mn(II) and Zn(II) showed only slight tendency to form mixed-ligand complexes containing $oxac^{2-}$ and acetate, but Mg(II) in 50% dioxane was found to form unusually stable mixed-ligand complexes, $Mg(OAc)oxac^-$ and $Mg(OAc)_2oxac^{2-}$. This behavior appears to be associated with an anion-induced change in the coordination geometry of the central metal ion and is also manifested in the stepwise formation constants for the formation of $Mg(OAc)_2$ and $Mg(OAc)_3^-$. $Mg(OAc)_2(oxac^{2-})$ decarboxylates more slowly than Mg(oxac) and also shows catalysis by HOAc. Tautomerization rate studies show that ketonization of complexed $oxac_{enol}$ is slower in 50% dioxane than in H_2O, but uncomplexed enol ketonizes faster in the lower polarity solvent. A high value for the proton-catalyzed rate of enolization of $Zn(oxac)_{keto}$ in 50% dioxane suggests that the keto oxygen atom is not closely associated with the metal ion in this complex.

Metal-ion-catalyzed decarboxylation of oxalacetate (oxac) and its derivatives has elicited interest for many years owing to the strong resemblance to analogous reactions catalyzed by certain metalloenzymes.[1] The model reactions are generally accepted to procede via the formation of a five-membered chelate which loses CO_2 to yield a complex of pyruvate enolate as the immediate reaction product.[1,2]

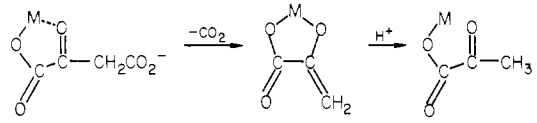

1 2 3

A dead-end side path arises from the enolization of **1** followed by metal ion addition and proton loss to give an inert dinuclear complex.[3,4]

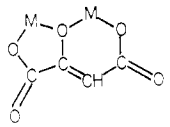

4

The catalytic effectiveness of divalent metal ions at low concentrations has been observed to be greatly enhanced in solvents having a lower polarity than water,[5-8] and because enzyme active sites present regions surrounded by hydrophobic groups, studies in mixed-solvent systems have been deemed especially attractive as enzyme models. Tsai in particular has expounded on this thesis.[7]

In early work, Kosicki and Lipovac[5] examined catalysis by Mg^{2+} and Mn^{2+} in ethanol–water mixtures. The stability constants of the M^{2+}–$oxac^{2-}$ complexes were observed to increase as the proportion of ethanol in the solvent mixture was increased, but the decarboxylation rate constants were found to be little influenced by the solvent. Tsai, Tsai, and Samad[6] examined Mn^{2+} catalysis in dioxane–water mixtures and found that the rate–metal ion concentration profiles did not show simple saturation kinetics but displayed a more complicated dependence. In more recent work,[7] Tsai studied the influence of ethanol on the Mn(II)-catalyzed decarboxylation rates of oxac in acetate buffers at "pH 5.1". Essentially in agreement with Kosicki and Lipovac,[5] only small increases in rates were observed as the solvent polarity was reduced.

On the surface, the small influence of solvent on the rates seems to argue against the above mechanism which requires that in the transition state negative charge be transferred from the 4-carboxylate group to an atom lying in the primary coordination sphere of the cation. Thus, a decrease in the solvent dielectric constant should be accompanied by an increase in rate. To explain this discrepancy, Kosicki and Lipovac[5] proposed that several factors may adversely interfere with an assessment of the true reaction rate in solvents of low polarity: conversion of oxac from the active keto to the inactive enol, association of the catalytic cation with other anions present in solution, and decreased proton dissociation of oxac. Some evidence that enolization may be responsible for low rates was provided by Rund and Plane,[9] who noted that both the formation constant and rate constant for the decarboxylation of the Ni(II) complex of 3,3-dimethyloxalacetate were higher in 20% dioxane than in an aqueous solution employing acetate at the same buffer ratio.

In principle it should be possible to correct for the interfering effects postulated by Kosicki and Lipovac, but none of these earlier studies were sufficiently exhaustive to allow these factors to be evaluated. Of particular importance, in none had the influence of pH been investigated. The pH not only determines the distribution of oxac between the slowly reacting protonated forms and the active keto complex but it also determines the distribution between the keto and inactive enolate complex.[3,4] Furthermore, in those studies where a buffer was employed, increased complexation between the catalyst and the anionic buffer component at low solvent polarities was not taken into account.

(1) For a review see R. W. Hay, "Metal Ions in Biological Systems", H. Sigel, Ed., Vol. 5, Marcel Dekker, New York, 1976.
(2) R. Steinberger and F. H. Westheimer, *J. Am. Chem. Soc.*, **73**, 439 (1951).
(3) W. D. Covy and D. L. Leussing, *J. Am. Chem. Soc.*, **96**, 3860 (1974).
(4) N. V. Raghavan and D. L. Leussing, *J. Am. Chem. Soc.*, **98**, 723 (1976).
(5) George W. Kosicki and Stanislava N. Lipovac, *Nature (London)*, **200**, 359 (1963).
(6) C. S. Tsai, Y. H. Tsai, and R. A. Samad, *Biochem. J.*, **124**, 193 (1971).
(7) C. S. Tai, Y. T. Lin, C. Reyes-Zamora, and J. A. Fraser, *Bioinorg. Chem.*, **4**, 1 (1974).
(8) P. R. Bontchev and V. Michaylova, *J. Inorg. Nucl. Chem.*, **29**, 2945 (1967).
(9) John V. Rund and Robert A. Plane, *J. Am. Chem. Soc.*, **86**, 367 (1964).

0020-1669/81/1320-4240$01.25/0

Table I. Logarithms of the Constants for the Protonation of Oxalacetate and Acetate and for the Formation of the Metal(II) Acetate Complexes (25 °C; I = 0.10)

equilibrium	% dioxane (v/v) 0	25	50	75
$[HOxac^-]/[H^+][oxac^{2-}]$	4.03	4.58	5.40	6.10
$[H_2OXac]/[H^+][Hoxac^-]$	2.35	2.68	3.22	4.11
$[HOAc]/[H^+][OAc^-]$	4.53	5.10	5.99, 6.03[a]	7.23
$[ZnOAc^+]/[Zn^{2+}][OAc]$	1.0[b]	1.45	2.20, 2.32[a]	3.20
$[Zn(OAc)_2]/[ZnOAc^+][OAc^-]$	0.81[c]		1.29	
$[MnOAc^+]/[Mn^{2+}][OAc^-]$	1.0[d]	1.42	1.91, 1.97[e]	2.18
$[Mn(OAc)_2]/[MnOAc^+][OAc^-]$			1.3	
$[MgOAc^+]/[Mg^{2+}][OAc^-]$	0.84[d]		2.4[f]	
$[Mg(OAc)_2]/[MgOAc^-][OAc^-]$			2.6[f]	
$[Mg(OAc)_3^-]/[Mg(OAc)_2][OAc^-]$			2.5 ($\beta_3 = 10^{7.5}$)[f]	

[a] Reference 22. [b] Reference 31. [c] Reference 32 (20 °C). [d] Calculated from ref 33 with use of the Davies equation. [e] Reference 21. [f] Reference 18.

In the present study, we set out not only to correct for changes in the protonation of oxac and interference by buffer but also to determine the true rate constants for the decarboxylation of the keto complexes by correcting for the distribution of the oxac complexes between the keto and enol forms. We report here the results of an intensive investigation of the catalytic effects of Mg^{2+}, Mn^{2+}, and Zn^{2+} in 50:50 (v/v) dioxane–water mixtures. The results of briefer studies on 25:75 and 75:25 solvent mixtures are also presented, and comparisons with the aqueous solution behavior are made. The results provide pertinent information having a bearing on the reaction mechanism.

Experimental Section

Reagent grade 1,4-dioxane obtained from Chemical Samples Co. was refluxed with metallic sodium overnight and fractionally distilled before use. The purity of the distillate of dioxane was checked with the use of a Hewlett-Packard 5700a gas chromatograph. Oxalacetic obtained from ICN Pharmaceuticals, Inc., was determined to have a purity of 97% by titration with a standard NaOH solution. Stock solutions of $MnCl_2$ and $MgCl_2$ were prepared from the solid salts. $ZnCl_2$ solutions were prepared by dissolving reagent grade Zn metal in a known amount of hydrochloric acid. All of these metal ion solutions were standardized by titration with EDTA. Double-distilled water was used throughout.

The pH scale used was one in which the reading of a pH meter was converted to –log of hydrogen ion concentration. This scale was established for each of the solvent mixtures by determining the pH meter readings of solutions containing known concentrations of HCl at 25 °C. Each solution was adjusted to an ionic strength of 0.1 with KCl. Excellent linearity between the pH meter reading and the true pH was obtained in the range pH 2–5 for each solvent.

For each solvent mixture, the pK_a values of H_2(oxac) and HOAc and the stability constants of the M^{2+}–acetate complexes were determined via pH titrations at 25.0 °, I = 0.1. The values obtained are given in Table I.

Decarboxylation rates of oxac in 50% dioxane were determined as a function of pH. The reaction solutions were made about 10^{-5} M in EDTA to inhibit catalysis by adventituous metal ions. The rate constants resolved for the individual species are 1.8×10^{-5} s^{-1} [$oxac^{2-}$], 2.4×10^{-4} s^{-1} [$Hoxac^-$], and 3.7×10^{-5} s^{-1} [H_2oxac]. These values are similar to those determined in H_2O and in 25% and 75% dioxane mixtures. The overall uncatalyzed rates of decarboxylation are thus seen to be little influenced by the dioxane content of the solvent.

For the catalytic rate determinations, one of a pair of reaction solutions in a given solvent mixture was initially made up to contain known concentrations of divalent metal chloride and an acetic acid–acetate buffer. Sufficient KCl was added to bring the ionic strength of the final mixed solution to 0.10. A second solution was made up to contain about 0.2 mM oxac and had identical concentrations of buffer and KCl as the first solution. Adjustments of these solutions to identical pH values were made by the addition of HCl or NaOH as was necessary. Reactions were initiated by mixing equal volumes of the two reactant solutions. In 75% dioxane $NaClO_4$ was employed to adjust the ionic strength to obviate difficulties encountered with KCl. When the oxac concentration is maintained at low levels, the only oxac complexes that need be considered were those having a metal ion:ligand ratio of 1:1, or lower.

When oxac solutions are mixed with those containing a divalent metal ion, a biphasic absorbance change is observed in the UV region. An initial increase occurring over approximately 30 s. arises primarily from conversion of keto complexes to enol complexes.[1,3,10] A slower absorbance decrease requiring 10–30 min is a manifestation of decarboxylation. The rates of the faster absorbance changes were measured with a Durrum Gibson stopped-flow spectrophotometer interfaced to a NOVA minicomputer. For each kinetic run, 250 data points were logged at precise time intervals. The slower decarboxylation rates were followed spectrophotometrically and manometrically. Cary 14 and Gilford 250 spectrophotometers were employed for the slower optical determinations. Carbon dioxide evolution was followed in a sealed system connected to a Texas Instrument precision pressure gauge, Model 145-01, the output of which was logged with a strip chart recorder. It was verified that the pseudo-first-order rate constant for CO_2 evolution during the slow phase of the reaction was identical with the corresponding rate constant determined spectrophotometrically. This shows that the absorbance increase initially observed arises from processes that do not primarily involve CO_2 release; i.e., it arises primarily from tautomerization.

The reaction rates for the tautomerization and decarboxylation processes occur over sufficiently different time scales that each can be analyzed as a single exponential approach to an "infinite" time value. A least-squares computer fit of the time trace for the response of the particular instrument employed in a kinetic run was made with the use of eq 1 where R_t is the instrument response at time t, R_∞ is

$$R_t = R_\infty + R_1 e^{-tk_{i,obsd}} \quad (1)$$

the response at "infinite" time, R_1 is the amplitude of the signal, and $k_{i,obsd}$ is the experimentally determined pseudo-first-order rate constant for the process (i = 1, fast; i = 2, slow).

The intrinsic rate of decarboxylation of Mg(oxac) is sufficiently slow in 50% dioxane that it was feasible to estimate its overall stability constant directly with a spectrophotometric titration in solutions buffered with *N,N,N',N'*-tetramethylethylenediamine. The monoprotonated form of this diamine neither forms complexes with Mg^{2+} nor catalyzes the decarboxylation of $oxac^{2-}$, and the diamine itself only forms weak Mg^{2+} complexes. So that the formation of $Mg(oxac)_2$ could be suppressed, the Mg^{2+} concentration was varied at a level well in excess of $oxac^{2-}$, which was 5×10^{-5} M. From these experiments, the stability constant of Mg(oxac) was found to be $10^{2.83}$ M^{-1} in 50% dioxane. This compares very favorably with a value $10^{2.65}$ M^{-1} obtained kinetically. A pronounced increase in the absorbance of the solutions buffered at pH >8 indicated the formation of an enolate complex. The pK_a for $Mg(oxac) \rightleftharpoons Mg(oxacH_{-1})^- + H^+$ was found to be 8.7 in 50% dioxane. Earlier, for aqueous media, Kosicki and Lipovac[11] found a value of 7.4, while Tate et al.[12] reported 8.1 for this ionization.

H_2oxac in 100% dioxane has been reported to possess an enol content of 67%.[13] We have redetermined this value using a rapid Br_2 titration and obtained results falling in the range 68 ± 5%. From the measured intensity of the 262-nm maximum of H_2oxac in 100% dioxane and the assumption of 68% enol, a molar absorptivity of 1.1×10^4 M^{-1} cm^{-1} was calculated for H_2oxac_{enol}. This value of the molar absorptivity is in very close agreement with the value obtained by Hess and Reed[13] from studies utilizing NMR, UV, and IR measurements on oxac in various solvent mixtures. Evidence indicates that at the absorption maximum the molar absorptivity of $oxac_{enol}$ is independent of its degree of protonation or complexation[14] (if metal ion–ligand charge-transfer bands are absent). With use of the molar absorptivity determined above, the enol/keto ratios of protonated and unprotonated oxac in the various solvent mixtures of interest here were estimated from the itensities at the UV absorption maxima. The values given in Table

(10) A. Kornberg, S. Ochoa, and A. Mehler, *J. Biol. Chem.*, **174**, 159 (1948).
(11) George W. Kosicki and Stanislava N. Lipovac, *Can. J. Chem.*, **42**, 403 (1964).
(12) S. S. Tate, A. K. Grzybowski, and S. P. Datta, *J. Chem. Soc.*, 1381 (1964).
(13) J. L. Hess and R. E. Reed, *Arch. Biochem. Biophys.*, **153**, 226 (1972).
(14) S. S. Tate, A. K. Grzybowski, and S. P. Datta, *J. Chem. Soc.*, 1372 (1964).

Table II. Percent Enol of Oxalacetic Acid in Dioxane-H_2O Mixtures[a]

	v/v % dioxane				
species	0	25	50	75	100
$oxac^{2-}$	12	20	24	20	
$Hoxac^-$	11	18	20	44	
H_2oxac	6	12	24	43	68

[a] Calculated with the assumption ϵ_{max} enol = 1.1×10^4 M^{-1} cm^{-1}.

II are estimated to have about 10% uncertainties. In general, the enol/keto ratio is seen to increase as the percentage of dioxane in the solvent mixture increases. The very low enol content of H_2oxac in 0 and 25% dioxane likely arises from the very high degree of hydration which occurs in these solvents.[15-17]

The enol/keto ratios of the M(oxac) complexes, K_M^{enol}, may be estimated spectrophotometrically provided the fraction of enol is not too high and the intrinsic rate of decarboxylation of the keto complex is slow relative to the rate of tautomerization. The first condition arises because the keto content is obtained by difference and its estimation is subject to large errors when the enol is predominant. The second condition arises because at the time when the metal ion catalyst and oxac are first mixed the keto complex is formed at a relatively high concentration. If the decarboxylation rate constant has a value comparable to, or greater than, that for enolization, appreciable concentrations of oxac may undergo decarboxylation before the competing enol/keto equilibrium is established. This may lead to a low spectrophotometric estimation of the enol content. As an example, the results obtained here show that in 50% dioxane up to 30% of the oxac may be lost within the first 30 s after mixing with Zn(II). By the end of the initial reaction period, CO_2 evolution becomes very slow because the active keto complex is present at a low concentration and the enol complex is predominant.

Of the complexes examined here in 50% dioxane, Mg(oxac) is the only one for which the spectrophotometric estimation of the enol content is feasible. From the absorptivity of 6.7×10^3 M^{-1} cm^{-1} determined at its 278-nm maximum and the assumption of a value of 1.1×10^4 M^{-1} cm^{-1} for the molar absorptivity of the enol form, a value of 1.6 was obtained for $K_{Mg(oxac)}^{enol}$ in 50% dioxane. Correcting for 10–15% decomposition of the oxac during the preequilibration period yields a value of about 1.8 for the enol/keto ratio.

Fortunately when the spectrophotometric estimation becomes grossly inaccurate, as is the case with Mn(oxac) and Zn(oxac) in 50% dioxane, the enol/keto ratios may be resolved from the concentration dependence observed for the faster of the biphasic processes. The means by which these are extracted from the data is described in the Appendix.

Results and Discussion

The stability constants shown in Tables I and III exhibit solvent dependencies that qualitatively can be interpreted on the basis of simple electrostatic interactions: as the solvent dielectric constant decreases, the attraction between oppositely charged particles increases. In Table I the protonation constants of $oxac^{2-}$ and OAc^- are each seen to increase by about 1.4 log units in going from H_2O to 50% dioxane while the protonation constant of $Hoxac^-$ increases by slightly less than one unit. The stability constants of the metal ion–acetate complexes are also seen to be higher by 1 order of magnitude in the semiaqueous medium. Caution should be exercised in interpreting this increment, however, because the aqueous values were taken from the literature and had been determined under somewhat different conditions than employed here. The stepwise constant for the formation of $Zn(OAc)_2$ also shows an increase in the dioxane mixture, but, as expected for lesser charge interaction, the increment amounts to only 0.5 log units. In both solvents, complexation by Zn(II) and acetate shows

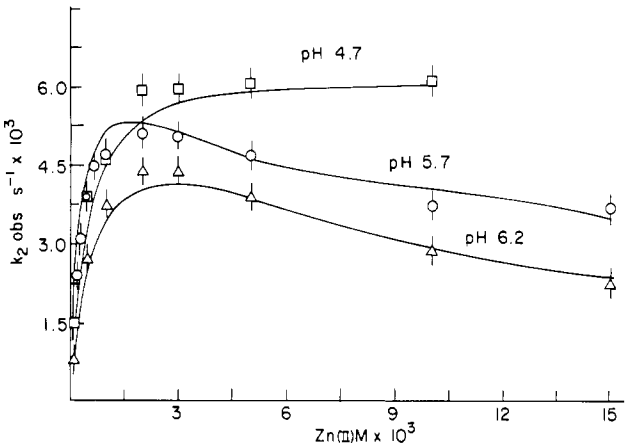

Figure 1. Representative slow rate–concentration profiles for Zn(II)-catalyzed decarboxylation. The solid lines are theoretical.

normal behavior in the sense that the order of the stepwise constants is $K_1 > K_2$.

In contrast to the behavior of Zn(II), the second and third stepwise constants for the formation of $Mg(OAc)_2$ and $Mg(OAc)_3^-$ in 50% dioxane are at least as large as K_1.[18] This causes the higher complexes to be formed simultaneously with $Mg(OAc)^+$, and in this situation the value of K_2 cannot be determined accurately. Hoffman[19] has reported that K_2 for the formation of $ZnCl_2$ in methanol is slightly larger than K_1 and has attributed the inversion to a change in coordination geometry from octahedral in the 1:1 complex to tetrahedral in the 1:2 complex. It is possible that a similar change in coordination number and geometry accounts for the behavior of Mg(II) in 50% dioxane. An important implication of this solvent effect on stabilities is that studies on metal ion–ligand interactions in aqueous media may not provide very good models for the behavior in a less polar enzyme environment.[20]

Complexing by the Cl^- present in our 50% dioxane solutions does not seem to be significant at the concentrations employed. The stability constants obtained here for $Zn(OAc)^+$ and $Mn(OAc)^+$ are in excellent agreement with those determined by Sigel[21,22] for 50% dioxane solutions in the presence of ClO_4^-. Likewise, a redetermination of the Mg^{2+}–OAc^- formation constants using ClO_4^- in place of Cl^- yielded essentially the same values as given in Table I.[18] In 75% dioxane, however, interference by Cl^- necessitated using $NaClO_4$ as the inert electrolyte.

The reaction rates in 50% dioxane were found to be qualitatively similar to those observed for aqueous media.[3,4] Representative rate constants for the slow loss of CO_2 are shown in Figure 1 as a function of the Zn(II) concentration. At low Zn(II) concentrations, the positive slopes indicate the formation of 1:1 complex that loses CO_2, and the negative slopes at the higher Zn(II) concentrations in the less acidic media arise from the formation of the polynuclear complex. Similar behavior was also observed with Mn(II) and Mg(II) except that the last ion gave no indication for the formation

(15) F. C. Kokesh, *J. Org. Chem.*, **41**, 3593 (1976).
(16) C. I. Pogson and R. G. Wolfe, *Biochem. Biophys. Res. Commun.*, **46**, 1048 (1972).
(17) Mark Emly and Daniel L. Leussing, *J. Am. Chem. Soc.*, **103**, 628 (1981).
(18) The Mg^{II}–OAc^- stability constants in 50% dioxane were determined titrimetrically in our laboratories by Lai-Duien Yuen.
(19) (a) H. Hoffmann, G. Platz, and M. Franke, *Proc. Int. Conf. Coord. Chem., 16th*, 3.35 (1974); (b) H. Hoffmann, *Pure Appl. Chem.*, **41**, 327 (1975).
(20) R. J. Irving and W. C. Fernelius, *J. Phys. Chem.*, **60**, 1427 (1956), also describe a reversal in the values of K_1 and K_2 for complex formation in 50% dioxane.
(21) H. Sigel, R. Griesser, B. Prijs, D. B. McCormick, and M. G. Joiner, *Arch. Biochem. Biophys.*, **130**, 514 (1969).
(22) R. Griesser, B. Prijs, and H. Sigel, *Inorg. Nucl. Chem. Lett.*, **4**, 443 (1968).
(23) E. Gelles and R. W. Hay, *J. Chem. Soc.*, 3673 (1958); E. Gelles and A. Salama, *ibid.*, 3683, 3689 (1958).

Table III. Overall Constants for Moxac Complexes in Dioxane–H_2O Mixtures (25 °C; I = 0.10; oxac = $oxac_K$ + $oxac_E$)

% dioxane	reaction	log β'
0	$Mg^{2+} + oxac^{2-} \rightleftharpoons Mg(oxac)$	1.02
	$Mg(oxac) \rightleftharpoons Mg(oxacH_{-1})^- + H^+$	~7.6
	$Mg(oxac) \rightarrow CO_2 + \ldots$	$k'_M{}^{CO_2} = 0.0016\ s^{-1}$
	$Mn^{2+} + oxac^{2-} \rightleftharpoons Mn(oxac)$	1.58
	$2Mn^{2+} + oxac^{2-} \rightleftharpoons Mn_2(oxacH_{-1})^+ + H^+$	−3.67
	$Mn(oxac) \rightarrow CO_2 + \ldots$	$k'_M{}^{CO_2} = 0.0034\ s^{-1}$
	$Zn^{2+} + oxac^{2-} \rightleftharpoons Zn(oxac)$	2.34
	$2Zn^{2+} + oxac^{2-} \rightleftharpoons Zn_2(oxacH_{-1})^+ + H^+$	−1.16
	$Zn(oxac) \rightarrow CO_2 + \ldots$	$k'_M{}^{CO_2} = 0.0079\ s^{-1}$
25	$Mn^{2+} + oxac^{2-} \rightleftharpoons Mn(oxac)$	2.52
	$2Mn^{2+} + oxac^{2+} \rightleftharpoons Mn_2(oxacH_{-1})^+ + H^+$	−2.50
	$Mn(oxac) \rightarrow CO_2 + \ldots$	$k'_M{}^{CO_2} = 0.0043\ s^{-1}$
	$Zn^{2+} + oxac^{2-} \rightleftharpoons Zn(oxac)$	3.38
	$2Zn^{2+} + oxac^{2-} \rightleftharpoons Zn_2(oxacH_{-1}) + H^+$	0.07
	$Zn(oxac) \rightarrow CO_2 + \ldots$	$k'_M{}^{CO_2} = 0.0077\ s^{-1}$
50	$Mg^{2+} + oxac^{2-} \rightleftharpoons Mg(oxac)$	2.67, 2.83[a]
	$Mg(oxac) + OAc^- \rightleftharpoons Mg(OAc)(oxac^-)$	~2.9
	$Mg(OAc)oxac + OAc^- \rightleftharpoons Mg(OAc)_2(oxac^{2-})$ [b]	~2.8
	$Mg(oxac) \rightleftharpoons Mg(oxacH_{-1})^- + H^+$	−8.93[a]
	$Mg(oxac)$, $Mg(OAc)oxac^-$ $\rightarrow CO_2 + \ldots$	$k'_M{}^{CO_2} = 0.005\ s^{-1}$
	$Mg(OAc)_2oxac^{2-} \rightarrow CO_2 + \ldots$	$k'_M{}^{CO_2} = 0.0020\ s^{-1}$
	$Mg(OAc)_2oxac^{2-} + HOAc \rightarrow CO_2 + \ldots$	$k'_M{}^{CO_2} = 0.029\ M^{-1}\ s^{-1}$
	$Mn^{2+} + oxac^{2-} \rightleftharpoons Mn(oxac)$	3.44
	$Mn(oxac) \rightleftharpoons Mn(oxacH_{-1}) + H^+$	−6.76
	$Mn(oxac) \rightarrow CO_2 + \ldots$	$k'_M{}^{CO_2} = 0.0053\ s^{-1}$
	$Mn(oxac) + HOAc \rightarrow CO_2 + \ldots$	$k'_M{}^{CO_2} = 0.04\ M^{-1}\ s^{-1}$ (?)
	$Zn^{2+} + oxac^{2-} \rightleftharpoons Zn(oxac)$	4.40
	$2Zn^{2+} + oxac^{2} \rightleftharpoons Zn_2(oxacH_{-1})^+ + H^+$	0.81
	$2Zn^{2+} + oxac^{2-} + OAc^- \rightleftharpoons Zn_2(OAc)(oxacH_{-1} + H^+$	2.92
	$Zn(oxac) + OAc^- \rightleftharpoons Zn(OAc)(oxac)^-$	0.8 (?)
	$Zn(oxac) \rightarrow CO_2 + \ldots$	$k'_M{}^{CO_2} = 0.0069\ s^{-1}$
	$Zn(OAc)(oxac) \rightarrow CO_2 + \ldots$	$k'_M{}^{CO_2} = 0.006\ s^{-1}$ (?)
75	$MnOAc_? + oxac^{2-} \rightleftharpoons Mn(OAc)_?(oxac)$	4.33
	$2MnOAc_? + oxac^{2-} + OAc^- \rightleftharpoons Mn_2(OAc)_?(oxacH_{-1}) + H^+$	1.12
	$Mn(OAc)_?(oxac) \rightarrow CO_2 + \ldots$	$k'_M{}^{CO_2} = 0.0043\ s^{-1}$
	$ZnOAc_? + oxac^{2-} \rightleftharpoons Zn(OAc)_?(oxac)$	5.69
	$2ZnOAc_? + oxac^{2-} \rightleftharpoons Zn_2(OAc)_?(oxacH_{-1}) + H^+$	5.12
	$Zn(OAc)_?(oxac) \rightarrow CO_2 + \ldots$	$k'_M{}^{CO_2} = 0.008\ s^{-1}$

[a] Spectrophotometric value. [b] $Mg^{2+} + 2OAc^- + oxac^{2-} \rightleftharpoons Mg(OAc)_2(oxac^{2-})$, $\log \beta_3 = 8.32$.

of a polynuclear complex. Neglecting for the present the preequilibrium distribution of keto and enol species, the overall reaction sequence is consistent with that shown in Scheme I.

The values of the overall rate parameters obtained from a nonlinear curve-fitting procedure based on Scheme I are given in Table III. With Zn(II) in 50% dioxane, it is seen that decarboxylation is mediated primarily by the formation of Zn(oxac), but a minor contribution from the mixed-ligand complex, $Zn(OAc)(oxac)^-$ has also been found to be present. The binding of OAc^- to Zn(oxac) is weak, and the presence of the OAc^- in the primary coordination sphere of the metal ion has little influence on the rate of decarboxylation. The dinuclear complex, which is positively charged in aqueous media, is further stabilized in 50% dioxane by association with an OAc^- ion. Qualitatively, similar results were obtained for studies on Mn(II) catalysis. Quantitatively, Mn(II) forms weaker complexes that decarboxylate more slowly than those of Zn(II), just as is observed in aqueous media.

In contrast to the behavior noted for Mn(II) and Zn(II), Mg(II) in 50% dioxane displays important decarboxylation pathways involving the mixed-ligand complexes. An excellent fit to the data was obtained by assuming that both $Mg(OAc)(oxac)^-$ and $Mg(OAc)_2(oxac)^{2-}$ are formed and the former has the same decarboxylation rate constant as Mg(oxac), but that for $Mg(OAc)_2(oxac)^{2-}$ differs. The values found are given in Table III. It is also significant that the stability constants reported in Table III show that Mg(oxac)

Scheme I

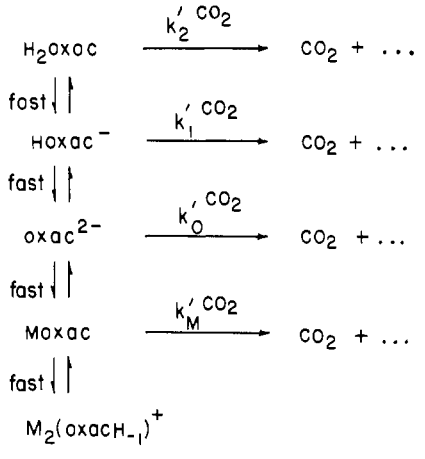

binds two OAc^- ions with almost identical stepwise constants. $oxac^{2-}$ and OAc^- appear to behave similarly as far as coordination to Mg(II) is concerned, and this suggests that $oxac^{2-}$ serves as a monodentate ligand.

$Mg(OAc)_2(oxac^{2-})$ was found to decarboxylate at half the rate observed for Mg(oxac) and also to show a pathway involving HOAc catalysis. We tentatively interpret this as showing that the two bound OAc^- ions interfere with the chelate ring closure by the pyruvate enolate that is formed as

Table IV. Rate and Equilibrium Constants for the Tautomerization of Oxalacetate

$$\text{keto} + \text{catalyst} \underset{k^E}{\overset{k^K}{\rightleftharpoons}} \text{enol} + \text{catalyst}$$

		H_2O			50% dioxane		
catalyst	species	K^{enol}	k^K, M^{-1} s^{-1}	k^E, M^{+1} s^{-1}	K^{enol}	K^K, M^{-1} s^{-1}	K^E, M^{-1} s^{-1}
H^+	$oxac^{2-}$	0.075	9×10^2	1.2×10^4	0.32	2.8×10^4	8.8×10^4
	$Hoxac^-$				0.25	1.5×10^3	6×10^3
	H_2oxac				0.3	34	10^2
	Zn(oxac)	5	6.2×10^2	1.2×10^2	30	6×10^3	2×10^2
HOAc	$oxac^{2-}$	0.075	0.7	9	0.32	4.9	20
	Mn(oxac)	0.7	3.7	5.3	12	11	0.9
	Zn(oxac)	2	4.1	2.1	30	14	0.5
OAc^-	Mn(oxac)	0.7	1.1	1.6	12	32	3
solvent[a]	Mn(oxac)	0.7	0.04	0.05	12	0.26	0.02
	Zn(oxac)	5	0.11	0.02	30	0.11	0.004
	Mg(oxac)[b]	0.30			1.8		
	$Mg(Ac)_2$(oxac)				2		

[a] The values given are for the first-order rate constants (s^{-1}). [b] Spectrophotometrically determined from preequilibrium solutions.

CO_2 is lost from $oxac^{2-}$. This in turn is manifested as a decrease in the reaction rate. The rate apparently becomes so slow that acid catalysis is favorable: $Mg(OAc)_2oxac^{2-} + HOAc \rightarrow CO_2 + Mg(OAc)_2$(enolpyruvate) $+ OAc^-$. An analogous pathway was not observed with Zn(II), possibly owing to an intrinsically faster reaction rate and low affinity for OAc^-. Mn(II), on the other hand, also gave some indication of HOAc catalysis.

The overall stability constants and rate constants shown in Table III are the values obtained after corrections had been made for the influences of pH, metal ion concentration, and acetate binding on the reaction rates. In qualitative agreement with Koscicki and Lipovac,[5] the largest effect of altering the reaction medium is observed not on the rate constants but on the stability constants. The values of the stability constants show substantial increases as the dielectric constant is reduced. In contrast, the rate constants show diverse changes that are dependent on the metal ion. In going from H_2O to 50% dioxane, the rate constants for Mg(oxac) more than double in value, those for Zn(oxac) decrease slightly and those for Mn(oxac) show intermediate behavior. These differences are the result of a correlation between the true rate constants for the decarboxylation of the keto complexes, the values of $K_{M(oxac)}^{enol}$, and how this latter quantity determines the fraction of an M(oxac) complex present in the active keto form. These relationships are discussed in more detail in the Appendix.

Consideration of the keto $\rightleftharpoons$ enol transformations leads to the set of reactions summarized in Scheme II. The rate–concentration curves for the faster tautomerization reactions typically are found to have unusual shapes, displaying minima as shown in Figure 2 for Zn(oxac). At low metal ion concentrations, the reactions proceed for the most part along pathways involving uncomplexed oxac and are found to be the same for all metal ion systems investigated here. As the Zn(II) concentration is increased, the rates approach pathways involving only Zn(oxac). Under our reaction conditions, the metal ion independent tautomerization reactions were found to involve H^+ and HOAc catalysis of $oxac^{2-}$ and $Hoxac^-$ and H^+ catalysis of H_2oxac. Zn(oxac) was catalyzed by H^+, HOAc, and solvent, while Mn(oxac) was catalyzed by HOAc, ^-OAc, and solvent. The slight differences in rate laws between the two complexes arose from the different conditions employed in studying their enolization rates: the more stable Zn(oxac) complex was examined under somewhat more acidic conditions than were used for Mn(oxac). Thus H^+ catalysis could be detected for the former and OAc^- catalysis for the latter.

The shapes of the tautomerization rate–concentration profiles are very sensitive to the value of $K_{M(oxac)}^{enol}$ for a complex,

Scheme II

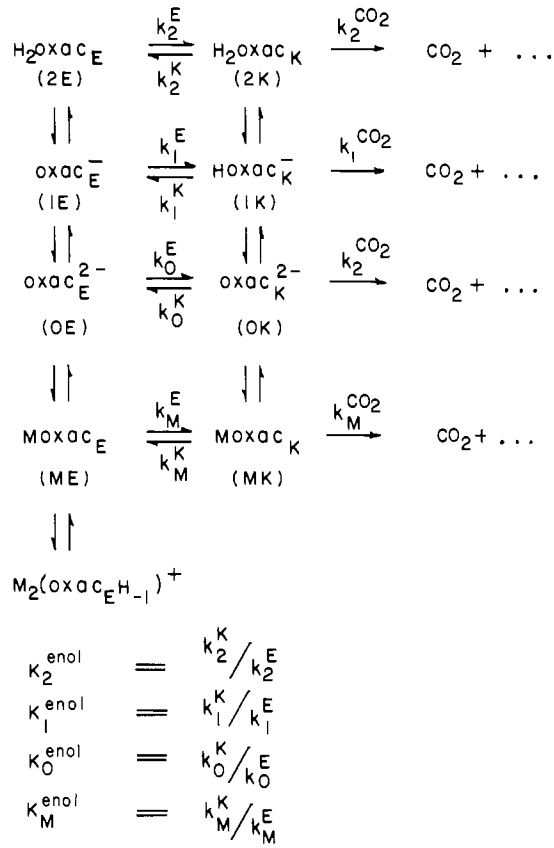

and this property enabled the enol/keto ratios to be evaluated kinetically. The dependence on $K_{M(oxac)}^{enol}$ is illustrated in Figure 2, where the solid and dashed curves represent the "best" fits obtained for values of $K_{Zn(oxac)}^{enol}$ equal to 30 and 10, respectively. The former curve is seen to fit the data points very well while the latter gives a poor fit. The calculations are described in the Appendix.

In Table IV the proton is observed in 50% dioxane to be a much better catalyst for enolization of both free and bound $oxac^{2-}$ than it is in H_2O. On the other hand, HOAc and solvent molecules are at best only slightly better catalysts in the mixed solvent. While the electrostatic attraction between H^+ and $oxac^{2-}$ is enhanced by lowering the dielectric constant, the neutral proton donors undergo an increase in pK_a and therefore do not show a substantial change in their interactions

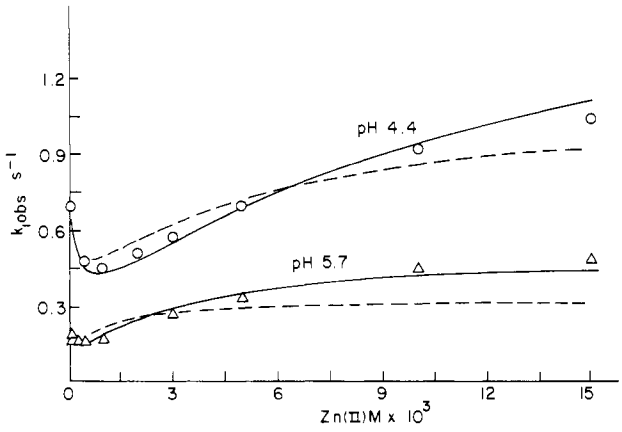

Figure 2. Representative fast rate–concentration profiles for tautomerization in the presence of Zn(II): solid line, "best" fit for $K_{Zn}^{enol} = 30$; dashed line, "best" fit for $K_{Zn}^{enol} = 10$.

Table V. Resolved Equilibrium Constants for the Formation of Keto and Enol Complexes and the Decarboxylation Rate Constants of $Moxac_K$

$$M^{2+} + oxac^{2-}{}_K \overset{\beta_K}{\rightleftharpoons} M(oxac)_K$$

$$M^{2+} + oxac^{2-}{}_E \overset{\beta_E}{\rightleftharpoons} M(oxac)_E$$

$$M(oxac_K) \xrightarrow{k_M^{CO_2}} CO_2 + \ldots$$

	H_2O			50% dioxane		
M(II)	log β_K	log β_E	$k_M^{CO_2}$, s^{-1}	log β_K	log β_E	$k_M^{CO_2}$, s^{-1}
Mg	0.96	1.29	0.0020	2.2	3.0	0.015
$Mg(OAc)_2$				2.9	3.7	0.006
Mn	1.41	2.11	0.0058	2.41	3.82	0.069
Zn	1.64	3.16	0.045	3.02	5.03	0.216

with $oxac^{2-}$. On the other hand, OAc^- is more basic in 50% dioxane and shows increased catalytic effectiveness toward Mnoxac.

Both the ketonization and enolization rates of uncomplexed $oxac^{2-}$ are faster in 50% dioxane. K_{oxac}^{enol} also increases because the increase in the enolization rate is larger than that for the back-reaction. The metal ion complexes also enolize faster in the dioxane mixture, but the ketonization rates are slower than in water. Thus, the metal ion kinetically stabilizes oxac enol; the more so, the lower the solvent polarity.

Thermodynamically, the increases in the values of $K_{M(oxac)}^{enol}$ brought about by reducing the solvent dielectric constant imply that the stabilities of the individual enol complexes increase more than those of the corresponding keto complexes. The magnitudes of these changes can be observed in Table V, where the formation constants calculated for the keto and enol species are given along with the true rate constants for the decarboxylation of the keto complexes. A transfer from H_2O to 50% dioxane causes the formation constants of the keto complexes to increase by 1–1.4 log units, while those for the enol complexes increase by about 1.7 log units.

The true rate constants for the decarboxylation of the $M(oxac)_{keto}$ complexes also show an increase as the solvent dielectric constant is reduced. In going from H_2O to 50% dioxane, 1 order of magnitude increase in the rate constant for CO_2 loss is gained by $Mg(oxac)_{keto}$ and $Mn(oxac)_{keto}$, while that for $Zn(oxac)_{keto}$ shows about a 5-fold increase. It is interesting to note that Zn(II) is as effective a catalyst in 50% dioxane as is Cu(II) in H_2O.[4]

The values of $k_M^{CO_2}$ correlate closely with those of $K_{M(oxac)}^{enol}$. This is demonstrated in Figure 3, where a plot of the logarithms of these two quantities is seen to define a straight line having a unit slope. Shown are values determined

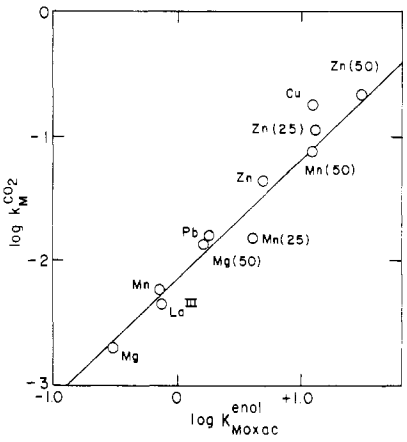

Figure 3. Relationship between the true rate constants for the decarboxylation of the keto complexes and the enol/keto ratios.

in this study along with those obtained earlier in our laboratory for other metal ions. Earlier Gelles and his co-workers[23] noted that the oxac decarboxylation rates correlate better with the stabilities of the oxalate complexes than with those of the oxac complexes. Because pyruvate enolate is isoelectronic with oxalate, they concluded that the transition state for decarboxylation occurs well along the reaction path toward the formation of the pyruvate enolate complex. The correlation implied in Figure 3 between the rate and the free energy of conversion of keto to enol strongly supports Gelles' postulate.

The stability constants of the keto complexes (Table V) show about the same solvent effects as those shown by the acetate complexes (Table I), indicating that the metal ion over a time average is essentially under the influence of only one of the $oxac^{2-}{}_{keto}$ carboxylate groups. Although chelate structure **1** is consistent with this observation, other evidence points to the possibility that **1** may not be the dominant structure in solution. For one, the similarities between the binding of $oxac^{2-}$ and ^-OAc to Mg(II) in 50% dioxane suggest that $oxac^{2-}$ behaves as a monodentate ligand. For another, the high value of the rate constant for the H^+-catalyzed enolization pathway of $Zn(oxac)_{keto}$ in 50% dioxane indicates that the keto oxygen atom in this complex is relatively free from the influence of the metal ion. If the increased stability of $Zn(oxac)_{keto}$ in going to 50% dioxane from water arises from the stabilization of **1**, the carbonyl group would lie more under the influence of the acidic metal ion and therefore should show a smaller tendency to accept a catalytic proton, contrary to the change observed in the rate constant. Still further evidence that chelate structure **1** comprises only a minor fraction of the keto complex has been obtained from studies on the NMR spectra of the Mn^{2+}[24] and lanthanide complexes[25] of pyruvate. No interaction between the keto group oxygen atom and the metal ion is evident. Owing to the additional electron-withdrawing properties of the 4-CO_2^- group, the keto group of $oxac^{2-}$ must be even a poorer electron donor than that of pyruvate and have a lower ability to displace an H_2O molecule from the primary coordination sphere of a metal ion.[26] Confirmatory evidence that the keto group of $oxac^{2-}$ is indeed more positive than that of pyruvate is obtained from the fact that the former ion is more highly hydrated.[17,27] On the basis of these consideration structures which seem more probably than **1** are the monodentate structures **5** and **6**, with **6**, in which the metal ion is located at the most basic site, likely the dominant one.[28]

(24) Albert S. Mildvan, *Acc. Chem. Res.*, **10**, 246 (1977).
(25) G. R. Choppin and R. E. Cannon, *Inorg. Chem.*, **19**, 1889 (1980).
(26) Owing to the very extensive hydration of H_2oxac, (ref 15) the pK_{1a} of oxac given in Table I is essentially that for the reaction $H_2oxac_{hyd} \rightleftharpoons H^+ + Hoxac^- + H_2O$. The pK_{1a} of H_2oxac_{keto} is at least 1 unit lower.
(27) M. Becker and H. Strehlow, *Z. Elektrochem.*, **64**, 813 (1960).

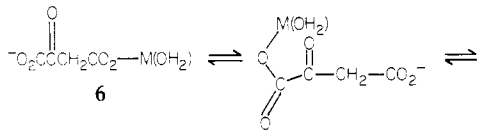

6 5

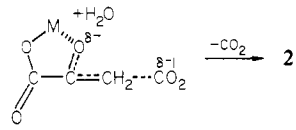

2

It is still possible for CO_2 loss to proceed via the formation of **1**; however, a reaction pathway analogous to those proposed[29,30] for acid- and base-catalyzed addition reactions to carbonyl groups appears as an attractive alternative. Here, the metal ion need not interact with the oxygen atom substituted on the 2-carbon atom until this oxygen atom has acquired sufficient electron density as CO_2 loss proceeds that it is able to displace an H_2O molecule from a metal ion coordination site. The oxygen atom substituted on the 2-carbon atom need only become as basic as a water molecule, and the trapping of the emerging enolate at this stage would very effectively drive the reaction in the forward direction. This mechanism is consistent with the evidence that activation arises primarily from the ability of the metal ion to stabilize pyruvate enolate.

Possible structures for the enol complexes are **7**, **8** and **9**.

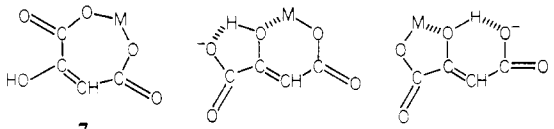

7 8 9

Molecular models show that the 1,4-coordinated structure, **7**, is quite feasible owing to the bond angles about the C=C group. Thus, the substantial metal-ion-induced increase in the enol content with decreasing dielectric constant may have its origins in a geometry favorable for the greatest charge neutralization. The enol coordinated structures **8** and **9** no doubt also make an appreciable contribution to the overall reaction. Not only is the enol oxygen atom inherently a better electron donor than the keto oxygen atom but the transfer of charge from the CO_2^- groups to the 2-oxygen atom via the carbon π system may also assist in the coordination of this group.

Acknowledgment. We wish to thank the National Science Foundation for a grant which supported this work.

Appendix

The relationship between the true rate constant for the decarboxylation of the keto complex, $k_M^{CO_2}$, and the overall value observed for the mixture of tautomers, $k'_M{}^{CO_2}$, is given by eq 1A. In the limit where $K_M^{enol} >> 1$, this equation

$$k'_M{}^{CO_2} = k_M{}^{CO_2}/(1 + K_M{}^{enol}) \quad (1A)$$

reduces to eq 2A. In the present study this limit is approached

$$K'_M{}^{CO_2} = k_M{}^{CO_2}/K_M{}^{enol} \quad (2A)$$

with Zn(II) catalysis. Owing to the correlation shown in Figure 3 between the two constants on the right hand side of eq 2A, solvent effects cancel and very small changes are noted for $k'_{Zn}{}^{CO_2}$. On the other hand, with Mg(II) in aqueous solutions $K_{Mg}^{enol} < 1$, so that changes in $k_{Mg}{}^{CO_2}$ are not entirely compensated for by corresponding changes in K_{Mg}^{enol}. Thus, the overall Mg(II) rate constants given in Table III show relatively large solvent effects. Although values of K_M^{enol} in themselves may change markedly with a variation in the solvent, these examples demonstrate that it is the value of the enol/keto ratio relative to 1, which determines the net effect on the overall reaction rate.

The individual equilibrium constants in Scheme II are related to the overall constants of Scheme I by

$$\beta_{1K} = \beta_1' \frac{\alpha_{MK}}{\alpha_K} \qquad [M^{2+} + oxac^{2-}{}_K \rightleftharpoons M(oxac)_K]$$

$$\beta_{1E} = \beta_1' \frac{\alpha_{ME}}{\alpha_E} \qquad [M^{2+} + oxac^{2-}{}_E \rightleftharpoons M(oxac)_E]$$

where $\alpha_{MK} = 1/(1 + K_M^{enol})$, $\alpha_K = 1/(1 + K_{ox}^{enol})$, $\alpha_{ME} = K_M^{enol}/(1 + K_M^{enol})$, and $\alpha_E = K_{ox}^{enol}/(1 + K_{ox}^{enol})$.

Two independent rate equations implied by Scheme II are eq 3A and 4A where $[oxac_K]_\Sigma = [0K] + [1K] + [2K] + [MK]$ and $[oxac_E]_\Sigma = [0E] + [1E] + [2E] + [ME] + [M_2EH_{-1}]$ and f_i is the fraction of a keto or enol species present as i at the completion of the first stage of the reaction, e.g., $f_{0K} = [oxac^{2-}{}_K]/[oxac_K]_\Sigma$, $f_{1e} = [Hoxac^-{}_E]/[oxac_E]_\Sigma$, etc.

$$\frac{-d[CO_2]}{dt} = (k_0{}^{CO_2}f_{0K} + k_1{}^{CO_2}f_{1K} + k_2{}^{CO_2}f_{2K} + k_M{}^{CO_2}f_{MK})[oxac_K]_\Sigma \quad (3A)$$

$$\frac{-d[oxac_E]_\Sigma}{dt} = -(k_{0K}{}^{K}f_{0K} + k_1{}^{K}f_{1K} + k_2{}^{K}f_{2K} + k_M f_{MK}) \times [oxac_K]_\Sigma + (k_0{}^{E}f_{0E} + k_1{}^{E}f_{1E} + k_2{}^{E}f_{2E} + k_M{}^{E}f_{ME})[oxac_E]_\Sigma \quad (4A)$$

Equations 3A and 4A may be expressed more concisely:

$$-d[CO_2]/dt = -k^{I}[oxac_K]_\Sigma$$

$$-d[oxac_E]_\Sigma/dt = -k^{II}[oxac_K]_\Sigma + k^{III}[oxac_E]_\Sigma$$

Casting in differential form and applying the condition that

$$0 = \delta[oxac_K]_\Sigma + \delta[oxac_E]_\Sigma + \delta[CO_2]$$

(as if CO_2 were not evolved from the solution phase) leads to eq 5A and 6A. From (5A) and (6A) can be derived the

$$\frac{-d\delta[CO_2]}{dt} = k^{I}(\delta[CO_2] + \delta[oxac_E]_\Sigma) \quad (5A)$$

$$\frac{-d\delta[oxac_E]_\Sigma}{dt} = k^{II}(\delta[oxac_E] + \delta[CO_2]) + k^{III}[oxac_E]_\Sigma \quad (6A)$$

relaxation matrix (7A). The solutions of (7A) are given in (8A).

$$\begin{vmatrix} k^{I} - \lambda & k^{I} \\ k^{II} & k^{II} + k^{III} - \lambda \end{vmatrix} = 0 \quad (7A)$$

$$\lambda_\pm = (k^{I} + k^{II} + k^{III} \pm [(k^{I} + k^{II} + k^{III})^2 - 4k^{I}k^{III}]^{1/2})/2 \quad (8A)$$

(28) In ref 7 the influence of Eu^{3+} on the ^1H NMR line shift of oxac is briefly described. The direction of the shift is said to indicate that the metal ion does not interact with the 4-CO_2^- group. This is a plausible result considering the experimental conditions employed. The ^1H NMR spectrum was obtained on a solution of 0.23 M oxalacetic *acid* containing an equimolar concentration of Eu^{3+}. We calculate that the pH was <<2, a situation in which the metal ion will find it difficult to compete with the proton for the most basic site on the $oxac^{2-}$ ion. Furthermore, the predominant form of oxac is H_2oxac and the influence of the extensive amount of hydrate present had not been considered in interpreting the line shifts. IR spectra of the solid Co^{2+} salt of 4-Et-$oxac^-$ described in ref 7 shows that in the solid the metal does interact with the 2-carboxyl group.

(29) William P. Jencks, *J. Am. Chem. Soc.*, **94**, 4731 (1972).
(30) J. Peter Guthrie, *J. Am. Chem. Soc.*, **102**, 5286 (1980).
(31) M. Yasuda, K. Yamsaki, and H. Ohtaki, *Bull. Chem. Soc. Jpn.*, **23**, 1067 (1960).
(32) R. S. Kolat and J. E. Powell, *Inorg. Chem.*, **1**, 293 (1962).
(33) D. W. Archer and C. B. Mark, *J. Chem. Soc.*, 3117 (1964).

The positive root corresponds to the pseudo-first-order rate constant for the faster process (mostly tautomerization) and the negative root corresponds to pseudo-first-order rate constant for the slower process (mostly decarboxylation).

Tautomerization is subject to general acid and base catalysis so each of the constants which pertain to a tautomerization rate in Scheme II is comprised of the sums of terms arising from various catalytic modes

$$k_i = k_{i\mathrm{H}}[\mathrm{H^+}] + k_{i\mathrm{HA}}[\mathrm{HA}] + k_{i\mathrm{A}}[\mathrm{A}] + k_{i\mathrm{H_2O}}[\mathrm{H_2O}] + \ldots$$

Certain terms in the complete rate expression are kinetically indistinguishable owing to a proton ambiguity, e.g., those for the pathways $\mathrm{Hoxac^-_K} + \mathrm{H_2O} \rightarrow \mathrm{Hoxac^-_E} + \mathrm{H_2O}$, and $\mathrm{oxac^{2-}_K} + \mathrm{H^+} \rightarrow \mathrm{oxac^{2-}_E} + \mathrm{H^+}$.

In analyzing the concentration and pH dependence of the $k_{i,\mathrm{obsd}}$ values, only one of the terms in such an equivalent set was retained. Further simplifications could be made in a series of experiments with a given metal ion because not all possible pathways were found to be present.

In performing the nonlinear curve fitting for a given data set, values of the rate constants for the various acid- and base-catalyzed enolization paths were estimated together with a value of $K_{\mathrm{M}}^{\mathrm{enol}}$ for the particular metal ion complex. The rate constants for the ketonization paths were then calculated. For each data point, an overall distribution of species was then calculated with use of the equilibrium constants given in Table III. This overall distribution was broken down into the contributions of each of the keto and enol species to obtain the necessary fractional distributions. These values were then substituted into (7A) together with the estimates of the rate constants, and a value of $\lambda+$ was calculated for that data point. Repeating this process the sum-squares $\sum(k_{i,\mathrm{obsd}} - \lambda_{+,\mathrm{calcd}})^2$, for all the data points were calculated and minimized by adjusting the values of the unknown rate constants and $K_{\mathrm{M}}^{\mathrm{enol}}$.

Registry No. H_2oxac, 328-42-7; Mn, 7439-96-5; Mg, 7439-95-4; Zn, 7440-66-6.

Contribution from the Chemistry Division, Argonne National Laboratory, Argonne, Illinois 60439

Rates of the Reactions of Uranium(VI) and the Hydrated Electron in Micellar Systems[1]

D. MEISEL, W. MULAC, and J. C. SULLIVAN*

Received May 15, 1980

The rate of the reaction between e_{aq}^- and U(VI) decreases with increasing sodium dodecyl sulfate (SDS) concentrations ≤4 mM and then remains constant up to 0.1 M SDS. The results are interpreted by the postulate of the interaction between U(VI) and premicellar aggregates of SDS. The rate of the reaction between the tris(carbonato)dioxouranium(VI) ion and the hydrated electron goes through a minimum and then increases with increasing cetyltrimethylammonium bromide (CTAB) concentration. A plausible mechanism that accounts for these observations is presented.

Introduction

The adsorption processes that occur at the interface between a suspended colloid and solution are important in the distribution of trace metal ions in natural aquatic systems.[2] When the metal ions under consideration can undergo oxidation–reduction reactions, it is of interest to assess the effect of such adsorption on the reactivity patterns of the metal ions.

The use of a micellar–water interface provides an opportunity to study the reactions of adsorbed ions in which the interactions are predominantly electrostatic and the structure of the adsorbent is at least moderately well-defined. In addition, by studying the dynamics of the redox reaction in concentrations less than cmc, it is conceptually possible to demonstrate differences between the homogeneous and heterogeneous reaction systems. Indeed, considerable effort has been devoted to the understanding of the effect of such micellar systems on the kinetics[4] of various processes.[3] Electron transfer across the double layer between many donor–acceptor couples has been studied in detail, most commonly following photoexcitation.[4] Similarly, reactions of aquated electrons, produced by radiolysis of micellar solutions, with acceptors of different affinities to the micelles were thoroughly studied.[5] Micellar effects on the rates of electron transfer to and from inorganic complexes have also been recently investigated.[6-9]

The results obtained in the present investigation use the reaction of e_{aq}^- with U(VI) to explore the above delineated areas of interest. The choice of U(VI) for the metal ion to be used was dictated by the interest in speciation of heavy metals in the aquatic environmental reservoir and the fact that the known chemistry of U(VI) permits a study of its interactions with both anionic and cationic micellar material.

Experimental Section

Reagents. The uranyl perchlorate stock solution was prepared by dissolving U_3O_8 in perchloric acid and recrystallizing and standardized by the usual gravimetric techniques. Sodium carbonate solutions were prepared by weight from an ultrapure solid. G. F. Smith perchloric acid was diluted and standardized by the usual techniques. Sodium

(1) Work performed under the auspices of the Office of Basic Energy Sciences of the U.S. Department of Energy.

(2) Parks, G. A. "Equilibrium Concepts in Natural Water Systems"; Gould, R. F., Ed.; American Chemical Society: Washington, D.C., 1967; pp 121–160.

(3) These were extensively reviewed in the following: (a) Fendler, J. H.; Fendler, E. J. "Catalysis in Micellar and Macromolecular Systems"; Academic Press: New York, 1975. (b) Cordes, E. H., Ed. "Reaction Kinetics in Micelles"; Plenum Press: New York, 1973. (c) Thomas, J. K. *Acc. Chem. Res.* **1977**, *10*, 133. Bunton, L. A. "Techniques of Chemistry"; Weissberger, A., Ed.; Wiley: New York, 1976; Vol. X, Part II. (e) Thomas, J. K.; Grieser, F.; Wong, M. *Ber. Bunsenges. Phys. Chem.* **1978**, *82*, 937.

(4) Cf.: (a) Grätzel, M. "Micellization and Microemulsions"; Mittal, K. L., Ed.; Plenum Press: New York, 1977; Vol. 2, p 531. (b) Kalyanasundaram, K. *Chem. Soc. Rev.* **1978**, *7*, 453. (c) Moroi, Y.; Infelta, P. P.; Grätzel, M. *J. Am. Chem. Soc.* **1979**, *101*, 573. Grätzel, M.; Thomas, J. K. *J. Phys. Chem.* **1974**, *78*, 2248, and references therein.

(5) See for example: (a) Wallace, S. C.; Thomas, J. K. *Radiat. Res.* **1973**, *54*, 49. (b) Fendler, E. J.; Fendler, J. H. *Adv. Phys. Org. Chem.* **1970**, *66*, 1472. (c) Patterson, L. K.; Grätzel, M. *J. Phys. Chem.* **1975**, *79*, 956. (d) Grätzel, M.; Kozak, J. J.; Thomas, J. K. *J. Chem. Phys.* **1975**, *62*, 1632. (e) Frank, A. J.; Grätzel, M.; Henglein, A.; Janata, E. *Ber. Bunsenges. Phys. Chem.* **1976**, *80*, 547.

(6) Bhalekar, A.; Engberts, J. *J. Am. Chem. Soc.* **1978**, *100*, 5914.

(7) Meisel, D.; Matheson, M. S.; Rabani, J. *J. Am. Chem. Soc.* **1978**, *100*, 117.

(8) Bruhn, H.; Holzwarth, J. *Ber. Bunsenges, Phys. Chem.* **1978**, *82*, 1006.

(9) Pelizzetti, E.; Pramauro, E. *Inorg. Chem.* **1979**, *18*, 882.

0020-1669/81/1320-4247$01.25/0